Tuning the Affinity for Lanthanides of Calcium Binding Proteins†

Ivano Bertini,*,‡ Ioannis Gelis,§ Nikolaos Katsaros,§ Claudio Luchinat,# and Alessandro Provenzani‡

Magnetic Resonance Center and Department of Chemistry, University of Florence, Sesto Fiorentino, Italy, NCSR Demokritos, Institute of Physical Chemistry, Agia Paraskevi Attikis, Greece, and Magnetic Resonance Center and Department of Agricultural Biotechnology, University of Florence, Sesto Fiorentino, Italy

Received March 27, 2003; Revised Manuscript Received May 16, 2003

ABSTRACT: The possibility of selectively substituting one or more lanthanides into the four canonical calcium binding sites of calcium-loaded vertebrate calmodulin (CaM) was investigated by monitoring changes in the ^{1}H-^{15}N HSQC NMR spectra of the ^{15}N-enriched protein upon titration with Yb^{3+}. The affinity of lanthanides for both N-terminal sites I and II is only moderately higher than that of calcium, and comparable with that of calcium for the two C-terminal sites. This situation induces binding of lanthanides to other noncanonical sites located at the interdomain linker, the N- and C-terminal ends, and at the inter-EF-hand linkers. Therefore, mutants were designed to alter the metal binding properties of calcium sites I (D22N, D24E), II (D58N, N60D, D58N−N60D), III (N97D), II−III (N60D−N97D), and IV (D129N), as well as of the inter-EF-hand linker of the N-terminal domain (N42K, T44K). The most striking effects were obtained for the N60D mutant at site II, as selective lanthanide binding is achieved even in the presence of excess calcium, and little or no population of the noncanonical sites occurs. Similar although less pronounced effects were observed for the N97D mutant. These findings allow us to better define some of the determinants of the relative affinities of calcium and lanthanides in CaM and, by extension, in other calcium binding proteins. Finally, by using CaM samples containing only three of the four calcium ions, it was possible to prepare well-defined Ca_3Ln-CaM derivatives (Ln = Tb, Dy, Tm, and Yb), with interesting properties as NMR probes.

Calcium binding proteins constitute the most abundant class of metalloproteins (*1*, *2*). This fact is related to the abundance of calcium as a metallic element on the earth crust and to its ability to interact with biomolecules. Nature exploits these properties by utilizing calcium(II) ions in many biological processes, from regulation of electric potentials to signal transduction (*3*, *4*). Calcium(II) concentration is high in the extracellular environment (around 1 mM) and much lower in the cells (around 1 μM) (*5*, *6*). This difference is maintained by active transport processes across the cell membranes, and is exploited in signal transduction through sudden openings of passive transport channels that cause calcium concentrations spikes (up to 10-fold increases) in the cytoplasm (*7*−*9*). In turn, these spikes cause the transient metalation of calcium binding proteins, which are triggered to activate a variety of functions (*10*−*12*). The signal is quenched by calcium buffering proteins (*13*, *14*), which then feed calcium ions to the active transport processes that pump excess calcium out of the cell (*15*). Both the thermodynamics and kinetics of calcium binding to cytoplasmic proteins have been tuned and optimized, during evolution, to the presence of micromolar concentrations of calcium in the resting state of cells. Similarly, the calcium proteins in the extracellular matrix have adapted to millimolar calcium concentrations, and processes such as cell adhesion and recognition are governed by calcium binding proteins that are sensitive to variations in calcium concentrations within the millimolar range (*16*). A variety of new processes and functions involving calcium binding proteins, both intra- and extracellular, are continuously discovered (*17*, *18*), and it is likely that the present knowledge of the role of calcium in biological processes represents but a small fraction of the whole picture.

Lanthanides are known to be spectroscopic probes for calcium-binding proteins. They are widely employed as luminescent probes (*19*, *20*) as well as NMR probes. In the latter case, their paramagnetism is exploited to generate new constraints in solution structure determinations (*21*−*27*). In view of these favorable properties, it would be desirable to have stoichiometrically definite and selectively substituted lanthanide-bound proteins (*28*). Apparently, this is sometimes a difficult goal, especially in the presence of multiple calcium binding sites. A typical system is provided by calmodulin (CaM)[1] (*29*). CaM and CaM-like proteins are constituted by four EF-hands pairwise connected by a flexible linker (*30*). The loop of each EF-hand contains a calcium binding site. Addition of lanthanides to calcium-loaded proteins sometimes provides selective lanthanide substitution (*31*). This is not the case for vertebrate CaM (*32*). Inspired by the cases in which selective substitution occurs, we have mutated CaM

† This work was supported in part by the EC contract No. HPRI-CT-1999-50006 (Transient NMR) and by Ente Cassa di Risparmio di Firenze.

* Author for correspondence: Prof. Ivano Bertini, Magnetic Resonance Center, University of Florence, Via Luigi Sacconi, 6, 50019 Sesto Fiorentino, Italy. Phone: +39055 4574272. Fax: +39055 4574271. E-mail: bertini@cerm.unifi.it.

‡ Magnetic Resonance Center and Department of Chemistry, University of Florence.

§ NCSR Demokritos.

Magnetic Resonance Center and Department of Agricultural Biotechnology, University of Florence.

10.1021/bi034494z CCC: $25.00
Published on Web 06/12/2003

in an attempt to provide Ca_3Ln-derivatives with one lanthanide selectively substituted in any of the four calcium binding sites. With this aim we have added Yb^{3+} to WT (wild type) and 10 mutants of calcium-loaded CaM and we have followed the Yb^{3+} binding through ^1H-^{15}N HSQC.

MATERIALS AND METHODS

Gene Cloning. The mammalian calmodulin gene was amplified by PCR from pRCB1 plasmid (*33*) and cloned into the commercial pET16B plasmid (NOVAGEN) (*34*). The latter plasmid carries a (His)10-tag before the MCS, followed by a Factor Xa restriction site. The ligation product was transformed in DH5α cells. The constructed plasmid pET16b-CaM was extracted from several clones and sequenced. Correctly sequenced clones were present.

Preparation of Mutants. pET16b-CaM was singly and doubly mutated at several positions as follows: D22N, D24E, N42K, T44K, D58N, N60D, D58N−N60D, N97D, N60D−N97D, D129N. The QuickChange site-directed mutagenesis kit (Stratagene) was used to mutate pET16b-CaM. The company protocol was followed. Several clones coming from each mutation reaction were sequenced.

Protein Expression and Purification. The procedure to obtain the wild-type calmodulin is described below and the same procedure was used for all mutants. pET16b-CaM was transformed in BL21(DE3)gold (NOVAGEN), and cells were grown at 37 °C and 130 rpm in 250 mL of LB medium containing 100 mg/mL ampicillin to an absorption of 0.8 at 600 nm. Cultures were centrifuged at 4 °C and 6000*g* for 10 minutes and the cell pellet was washed in 100 mL of M9 minimal medium (*35*). Cultures were centrifuged again at 4 °C and 6000*g* for 10 min and the cell pellet was resuspended in 250 mL of M9 minimal medium containing ^{15}N source, shaken at 37 °C and 130 rpm. After 1 h IPTG was added to a final concentration of 0.5 mM, and the cells were further incubated at 37 °C overnight (*36*). Cultures were then centrifuged at 4 °C and 6000*g* for 15 min and the cell pellet was resuspended in 20 mM MOPS, 300 mM NaCl, pH 8.0 (buffer A) and stored at −20 °C overnight. After the sample was thawed, the suspension was sonicated and centrifuged at 4 °C and 40 000 rpm in a Beckman Ultracentrifuge Ti70 rotor for 30 min. The soluble fraction containing the (His)-10-tagged recombinant protein was loaded onto an affinity column containing Ni−NTA resin (Qiagen) previously charged with Ni^{2+} and equilibrated with buffer A (*37*). The column was consecutively washed with buffer A until no 280 nm signal absorption was detectable and then with 20 mM MOPS, 300 mM NaCl, 10 mM imidazole, pH 8.0 (buffer B), again until no 280 nm absorption was detectable. Proteins attached to the column, including (His)10-tagged recombinant protein, were eluted with 20 mM MOPS, 300 mM NaCl, 150 mM imidazole, pH 8.0 (buffer C) until no 280 nm absorption was detectable. This protein fraction was concentrated to 1.5 mL with Centriplus cutoff 10000 Da (Millipore) and then buffer exchanged in 100 mM NaCl, 50 mM Tris-HCl, 1 mM $CaCl_2$ (pH 8.0) by a HiTrap 5 mL desalting column (Amersham pharmacia biotech). Restriction protease Factor Xa (Roche diagnostic) was added to the solution (30 μg of enzyme for 30 mg of recombinant protein) to cut the (His)10-tag. After incubation of the sample for 18 h at room temperature, the solution was incubated with 5% of Xarrest agarose resin (NOVAGEN) for 1 h to eliminate Factor Xa, and then loaded again onto the affinity column containing Ni−NTA resin (Qiagen) previously charged with Ni^{2+} and equilibrated with buffer A. The minor contaminant proteins were retained into the column and the recombinant protein without the (His)10-tag was eluted in buffer A. The purity was checked by SDS−PAGE in 15% polyacrylamide gels after staining of protein bands with Coomassie Blue R-250. Protein yield is about 25 mg/L for both wild type and mutant calmodulins. The recombinant WT and mutant proteins carry two extra amino acids compared to the native one, i.e., a His and a Met respectively at positions −1 and 0.

Sample Preparation. After protein purification, NMR samples were prepared by buffer exchange in Centricon cutoff 10000 Da (MILLIPORE). Samples were washed consecutively three times with a 20 mM EDTA solution pH 6.5 (to obtain the apo form and to remove any traces of Ni^{2+} ions), three times with a 20 mM MES, 400 mM KCl, 5 mM $CaCl_2$ pH 6.5 buffer (to reconstitute the fully Ca^{2+}-loaded form), and finally three times with a 20 mM MES, 400 mM KCl, pH 6.5 (loaded protein without Ca^{2+} excess). For most NMR experiments excess $CaCl_2$ was again added to each sample up to a final concentration of 10 mM. NMR samples (10% D_2O) were concentrated to about 1 mM protein solutions. Protein concentration was estimated by using a $\epsilon_{276} = 3300\ M^{-1}\ cm^{-1}$ (*38*). Native and mutant calmodulin samples were titrated with 50 mM solutions of analytical grade $LnCl_3$ (Sigma, Aldrich). Titrations were followed by 2D ^1H-^{15}N HSQC spectroscopy. The samples were kept at 4 °C between measurements.

NMR Spectroscopy. NMR spectra were acquired on Bruker AVANCE 700 and 600 spectrometers operating at 700.13 and 600.13 MHz, respectively, equipped with TXI gradient probes. The residual water signal was suppressed by either presaturation during both the relaxation delay and mixing time or gradient-tailored excitation (WATERGATE). The spectra were calibrated at different temperatures according to the empirical relationship $\delta_{H2O} = (-0.012T + 5.11)$ ppm, with T being the temperature (in °C). ^1H-^{15}N HSQC spectra were recorded for all lanthanide derivatives at 300 K using a spectral width of 16 and 32 ppm in the ^1H and ^{15}N dimensions, respectively. A total of 256 increments each with 1024 complex data points and 16 transients were collected. The recycle delays were in the range between 0.7 (paramagnetic) and 1.5 s (diamagnetic derivatives). Raw data were multiplied in both dimensions by a squared cosine window function and Fourier transformed to obtain a final matrix of 2048 × 2048, or of 512 × 512 real data points for the HSQC spectra. A polynomial baseline correction was applied in the f2 dimension. All NMR data were processed with the Bruker XWINNMR software packages. The program SPARKY (*39*)

[1] Abbreviations: CaM, calmodulin; HSQC, heteronuclear single-quantum coherence experiment; NMR, nuclear magnetic resonance; WT, wild type; (His)10-tag, 10 histidine tag; PCR, polymerase chain reaction; MCS, multicloning site; LB, Luria Bertani; IPTG, isopropyl-beta-D-thiogalactopyranoside; MOPS, 3-[*N*-morpholino]propanesulfonic acid; Ni−NTA, nickel nitrilotriacetic acid; SDS−PAGE, sodium dodecyl sulfate−polyacrylamide gel electrophoresis; EDTA, ethylenediaminetetraacetic acid; MES, 2-[*N*-morpholino]ethanesulfonic acid; $LnCl_3$, lanthanide chloride; CBCACONH, Cβ-Cα-carbonyl carbon-NH connectivity experiment; CBCANH, Cβ-Cα-NH connectivity experiment; NOESY, nuclear Overhauser effect spectroscopy; CaBP, calcium binding protein.

was used for analysis of the 2D spectra. Peak intensities were measured used the integration routine of SPARKY (*39*).

RESULTS

The present strategy to investigate the relative affinity of lanthanides for CaM and its mutants is based on ^{1}H-^{15}N HSQC titrations of ca. 1 mM solutions of calcium-loaded CaM (400 mM KCl, 20 mM MES, pH 6.5) with Yb^{3+} solutions *in the presence of 10 mM excess* Ca^{2+}. This experimental setup was arrived at as the safest in terms of lanthanide-binding properties and reproducibility. High ionic strength is known to decrease the relative affinity of lanthanides for noncanonical sites (see below) and to prevent precipitation (*19*, *40*). The relatively low pH value ensures that even transient formation of insoluble water-hydroxo lanthanide species is minimal at the concentrations used. Finally, the 10-fold calcium excess guarantees well-defined Ln/Ca competition conditions from one preparation to another. No excess calcium would require preparation of apo-CaM each time, and careful titration with Ca^{2+} up to exactly 4 equivalents. While this is feasible for WT CaM, some mutants could (and indeed have been found to) bind Ca^{2+} less well, so that at 4 equivalents some ill-controlled free Ca^{2+} could be present. The presence of Ca^{2+} in each of the four sites is easily checked by monitoring the signals of glycines 25, 61, 98, and 134. These glycines belong to each of the four EF-hand loops and their ^{1}H and ^{15}N downfield shift in the calcium-bound form is characteristic of a calcium-loaded site (*41*−*43*).

The binding of lanthanides was investigated by monitoring the paramagnetic effects on the protein ^{1}H-^{15}N HSQC peaks upon addition of increasing amounts of Yb^{3+} solutions. The interactions with the time-averaged magnetic moment of the paramagnetic lanthanide ion drastically affect the properties of the nuclear spins in its neighborhood. Specifically, in these experiments the nitrogen and proton nuclei of the peptide NH and side chain NH_2 groups experience (i) pseudocontact shift, which depends on the reciprocal third power of the metal−nucleus distance and on the polar coordinates of the nucleus within the frame of the metal magnetic susceptibility tensor, and (ii) line broadening, which depends on the reciprocal sixth power of the metal−nucleus distance (and is particularly strong for protons). These effects cause NH peaks within a certain distance from the metal center to be broadened beyond detection and, outside this shell, to be observable but shifted with respect to their position in the HSQC spectrum of the calcium derivative. Within the lanthanide series, these paramagnetic effects are smallest for Ce^{3+} and Eu^{3+} and largest for Tb^{3+} and Dy^{3+} ions. Yb^{3+} was chosen in this work as it has intermediate properties within the series: it causes signal disappearance within a shell of about 9 Å and measurable shifts up to 25 Å from the metal (*44*). Under such conditions, when Yb^{3+} is bound to a relatively strong EF-hand binding site some NH peaks are lost in the immediate neighborhood of the binding site itself, but several of the NH peaks from the neighboring site are still observable and shifted. Shifted peaks can be detected even relatively far from the binding site. On the other hand, lanthanides are known to bind more weakly to noncanonical sites (*19*, *40*), and their lifetime in those sites is expected to be sizably shorter than when bound to canonical sites. If the lifetime is still long compared to the difference in chemical shift of the neighboring nuclei in the bound and free form, but short compared to the transverse relaxation time of the signals in the free form, line broadening occurs also from these noncanonical sites, to an extent that can be even larger than the line broadening occurring in the fully bound form due to paramagnetic exchange broadening (*43*, *45*). As a consequence of exchange, it is possible that a peak from an NH group that is close to a noncanonical site becomes broadened even upon substoichiometric addition of the lanthanide.

For WT-CaM and for each of its mutants the lanthanide titrations described below showed both kinds of phenomena, i.e., (i) disappearance (without broadening) and reappearance of shifted (and broadened) peaks from NH groups in the vicinity of the canonical sites and (ii) early broadening and disappearance of peaks from NH groups in the vicinity of noncanonical sites. The titrations were extended beyond the first equivalent until possible, i.e., until excessive and generalized broadening occurred.

Titration of WT-CaM with Yb^{3+}. The ^{1}H-^{15}N HSQC spectrum of WT CaM (Figure 1A) is that of a single species with the full complement of four calcium ions. The assignment of the HSQC spectrum of CaM has been taken from literature (*46*) and independently checked under the present experimental conditions. Addition of Yb^{3+} to WT-CaM results in immediate strong perturbation of the HSQC spectrum. Already at 0.3 equivalents ($r = 0.3$) several NH signals belonging to the interdomain linker (78−81) are lost. Other signals coming from the ends of N- and C-termini (1−5 and 145−148) are broadened (Figure 2A). Some other signals decrease in intensity faster than expected from the stoichiometry of the titration. These signals (e.g., 42, 117) belong to residues located in the inter-EF-hand loops in both the N- and C-terminal domains. At the same time, the signals arising from the calcium binding sites I and II of the N-terminal domain begin decreasing in intensity, and new signals appear. At $r = 1$ the appearance of the HSQC spectrum is that of Figure 1B.

Several new peaks appear very early along the titration (e.g., A57′ in Figure 2A). They reach a maximum slightly above $r = 1$ and clearly belong to site II (some others reach a maximum beyond $r = 1.5$, are of low intensity and suffer soon from broadening (not shown)). They may be tentatively assigned to N-terminal domain signals arising from a species containing lanthanides at both sites I and II). Beyond $r = 1.5$, peaks from the C-terminal domain start decreasing in intensity, but no new peaks appear. Rather, a generalized broadening takes place beyond $r = 2$, which prevents the analysis of the last part of the titration.

A few observations can be made immediately: (i) there is little lanthanide selectivity for the canonical sites under the present experimental conditions; (ii) as noted previously (*32*), there is a preference for the N-terminal site I; (iii) the apparent lanthanide/calcium affinity ratio is larger than 1, but not high enough to prevent lanthanide binding to noncanonical sites. There are many such sites, located at the interdomain linker, at the N- and C-terminal ends, and at both inter-EF-hand loops. As discussed at the beginning of the results section, these sites apparently have shorter lifetimes than the canonical sites, so that the disappearance of the NH peaks is faster and more dramatic because of exchange broadening. As a consequence, it is not an easy

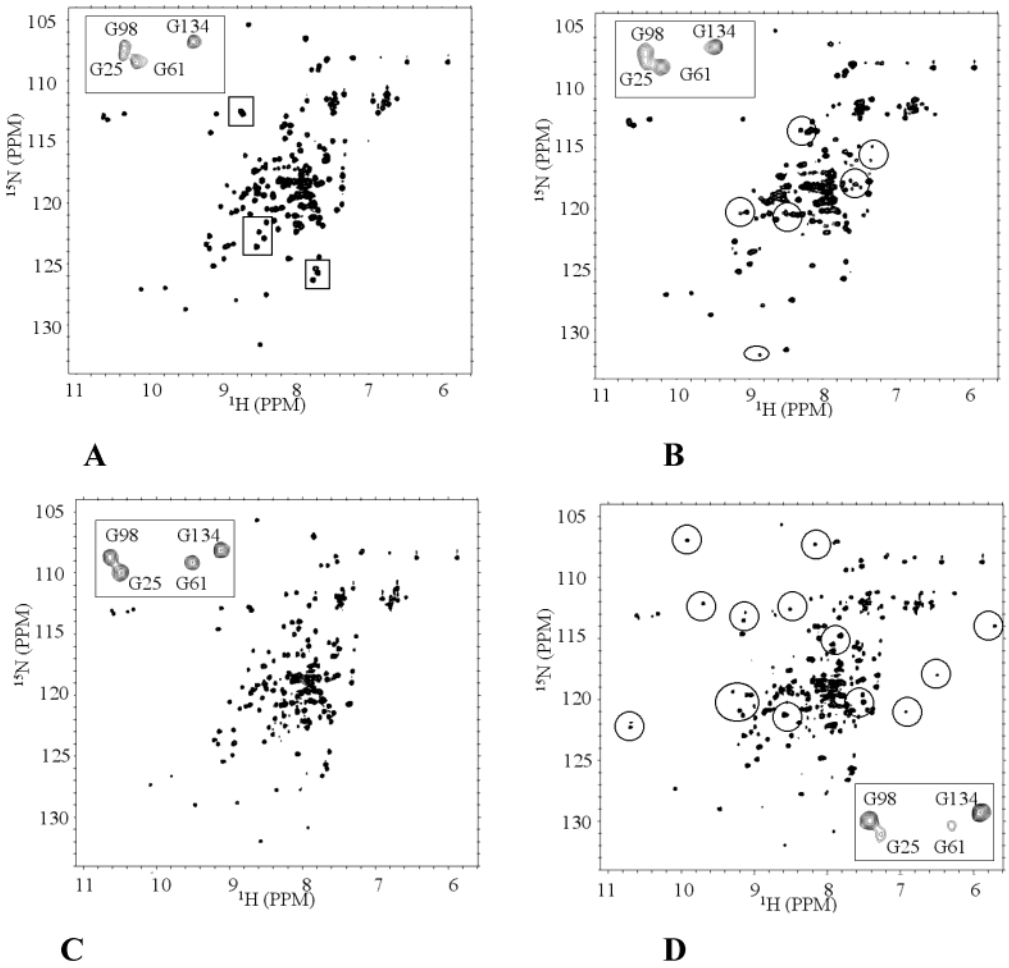

FIGURE 1: ^{1}H-^{15}N HSQC spectrum of calcium-loaded WT calmodulin in the absence (A) and in the presence of 1 equivalent of Yb^{3+} (B). The HSQC spectra under identical conditions of the calcium-loaded N60D mutant in the absence (C) and in the presence of 1 equivalent of Yb^{3+} (D) are also shown. The insets show enlargements of the region containing the peaks from the glycines 25, 61, 98, and 134 located at each of the four canonical sites. Note the disappearance in (A) but not in (C) of several peaks (in boxes) belonging to NH groups in the proximity of the noncanonical sites. Circles represent new pseudocontact-shifted peaks.

Scheme 1

1	2	3	4	5	6	7	8	9	10	11	12
D	x	(D/N)	x	(D/N)	x	x	x	x	x	x	E
+X		+Y		+Z		-Y		-X			-Z

task to mutate vertebrate CaM in such a way as to permit selective substitution of a lanthanide in any of the canonical sites while retaining the full complement of calcium in the other sites.

Choice of Mutants and Investigation Strategy. The consensus sequence for the canonical EF-hand sites is reported in Scheme 1. The calcium ligands are arranged in a roughly octahedral geometry, with donor atoms provided by the side chains of residues in the so-called +X, +Y, +Z, and −Z positions. Mutations at the −Z position were previously reported to strongly destabilize the metal binding site (*19*, *47*). Therefore, we concentrated on the other three positions, aiming at either changing the overall charge or the charge distribution of the site. One of these mutations was also planned with a residue having different side-chain length. In calmodulin, residues at the +X, +Y, and +Z positions are D−D−D, D−D−N, D−D−N and D−D−D in sites I, II, III, and IV, respectively. The planned mutations were D−D−D to D−N−D or D−D−E in site I, D−D−N to D−N−N, D−N−D or D−D−D in site II, D−D−N to D−D−D in site III, D−D−N to D−D−D in both sites II and III, and D−D−D to N−D−D in site IV. Two additional mutants were prepared carrying mutations on the loop between EF-hands I and II to eliminate one of the noncanonical sites.

The mutant HSQC spectra were assigned on the basis of the assignment of the WT. Most signals were superimposable to the WT signals, several other signals could be assigned unambiguously even if slightly shifted with respect to the WT, and only a few peaks were left unassigned in some mutants. For the N60D mutant an independent assignment based on ^{13}C-^{15}N 3D spectra was performed (CBCACONH, CBCANH, and ^{15}N−NOESY−HSQC, data not shown).

As the present approach relies on lanthanide titration performed in the presence of a ca. 10-fold excess free calcium ions with respect to the protein, the apparent lanthanide/calcium affinity ratio is decreased by 1−2 orders of magnitude with respect to the true one. This has the important consequence that non-negligible amounts of free lanthanide are present in solution along the titration, in turn favoring the binding of the lanthanide to noncanonical surface sites. The titration of the WT has shown that these surface sites are characterized by a much shorter lifetime than the

canonical sites, although not as fast as to provide signal averaging between free and lanthanide-bound species. Under these conditions, even small fractions of bound lanthanides can cause extensive line broadening due to exchange (*45*), and the latter can be taken as a sensitive indicator of the concentration of free lanthanide at any point of the titration. The free lanthanide concentration is inversely proportional to the apparent lanthanide/calcium affinity ratio for the canonical sites, so that this property can be exploited to rank the selected mutants in terms of their relative ability to bind lanthanides with respect to the WT.

Titration of CaM Mutants with Yb^{3+}. The behavior of the 10 CaM mutants upon addition of Yb^{3+} is summarized in Figure 2B−K, where for each mutant the intensity of selected ^{1}H-^{15}N HSQC cross-peaks is followed along the titration. As discussed above, in each titration two features are important to assess the changes in the apparent lanthanide/calcium affinity ratio for each canonical site. One is the behavior of the peaks arising from noncanonical sites. The earlier their broadening and disappearance, the lower the apparent lanthanide/calcium affinity ratio for one canonical site. The titration of the N42K and T44K mutants (Figure 2B,C) clearly showed the existence of one of these noncanonical site, i.e., the titration behavior was the same as that of the WT except for the disappearing rate of the peaks in the inter-EF-hand loop of the N-terminal domain that is the same as in the canonical first site. The other feature is the order of disappearance of the signals from the canonical sites, which shows the effect of a mutation on that particular site and the possible consequences on the neighboring sites.

All mutations except D129N result in a fully calcium loaded protein, with changes in the HSQC spectra with respect to the WT that are in most cases (D22N, N42K, T44K, D58N, N60D, N97D, N60D−N97D) limited to the immediate vicinity of the mutation. In the case of D24E and D58N−N60D, the alterations are more substantial and involve a large number of peaks from the N-terminal domain. In the D129N mutant, site IV does not contain calcium and the whole C-terminal domain is strongly affected and probably partially unfolded.

Upon addition of Yb^{3+} to both D22N and D24E mutants at the canonical site I the broadening and disappearance of peaks from all noncanonical sites increases, more dramatically for the latter (Figure 2D,E). Apparently, these mutations have decreased the apparent lanthanide/calcium affinity ratio of this site with respect to WT CaM. From the decrease in intensity of the peaks from the N-terminal site, it can be concluded that in D22N only the affinity for site I has decreased. On the other hand, in the D24E mutant a generalized broadening occurs at the N-terminal domain, indicating that the affinity for site I has decreased to the point that exchange broadening occurs also for this canonical site.

A more pronounced broadening of peaks from noncanonical sites is also seen for the D58N mutant (site II) (Figure 2F). As site I is still filled first in this derivative, we conclude that the mutation decreases the apparent lanthanide/calcium affinity ratio not only of site II but also of site I, so that the overall filling of the N-terminal domain sites is reduced. This situation is reverted in the double mutant D58N−N60D, which changes the consensus residues 1−3−5 in site II from D−D−N to D−N−D. In this mutant, the relative apparent affinity of the lanthanide for site II, and possibly also for site I, is even slightly higher than that of the WT as judged from the rate of decrease of the signals in the inter-EF-hand loop (Figure 2G).

At variance with the previous mutant, as well as with the WT and indeed with all other mutants described so far, upon Yb^{3+} addition to the N60D mutant (Figure 2H) a steady and linear decrease of the N-terminal peaks was observed, arising from both site I and site II. The same profile was followed by all the residues, including the residues coming from the inter-EF-hand loop of the N-terminal domain. This resulted in their disappearance around $r = 1$. No evidence of exchange broadening was seen for the N- and C-terminal ends, while residues arising from the interdomain linker decrease much more slowly than in WT, although still slightly faster than the N-domain residues. The HSQC spectra of the calcium-loaded N60D mutant and at the $r = 1$ point along the Yb^{3+} titration are shown in Figure 1C,D. Up to $r = 1$ the C-domain residues remained essentially unaffected, while they start decreasing above $r = 1$ and disappear around $r = 2.3$ (inter-EF-hand loop) or 3.5 (sites III and IV, not shown). This mutant is the first among the mutants described so far that succeeds in markedly enhancing the apparent lanthanide/calcium affinity ratio for one of the canonical sites, i.e., the N-terminal site II. This enhancement is strong enough that none of the noncanonical sites but the interdomain linker is appreciably populated until $r = 1$, and even the fraction of lanthanide bound to the interdomain linker is smaller than in WT, in such a way that the signals disappear only around $r = 0.6$. Another interesting feature of this mutant is that the increase in affinity for site II does not enhance appreciably the affinity for site I, so that site II is selectively filled.

The N97D mutation plays the same role of the N60D mutation but in site III. The titration (Figure 2I) shows that the broadening of peaks from the noncanonical sites is not abolished as in the N60D mutant but slightly decreased, indicating that one of the canonical sites has slightly higher lanthanide affinity than in the WT. This site is now site III, which becomes the first of the canonical sites to be populated, followed by the N-terminal sites in the same order as the WT. The selectivity, however, is not as high as for the N60D mutant. The double mutant N60D−N97D confirms that the effects are additive (Figure 2J). No evidence of exchange broadening from the noncanonical sites was present, and canonical site II was filled first, followed by site III and site I. Finally, the D129N mutant showed a behavior similar to the WT at the beginning of the titration, with exchange broadening from the noncanonical sites and filling of the N-terminal sites (Figure 2K). Before the complete filling of the N-terminal sites, all signals form the C-terminal domain start broadening and disappear soon after $r = 2$. This mutant thus behaves as an isolated N-terminal domain due to the impaired ability of the C-terminal domain to bind calcium both at the canonical and noncanonical sites.

Preparation of Ca_3LnCaM Derivatives of the N60D Mutant. As discussed at the beginning, all the conclusions drawn from the present mutants about the apparent lanthanide/calcium affinity ratio for the various sites refer to a situation in which the protein has the full complement of four calcium ions (with the exception of the D129N mutant) and the solution contains 10 mM excess Ca^{2+} ions. Under these conditions, after the addition of 1 equivalent of Yb^{3+}

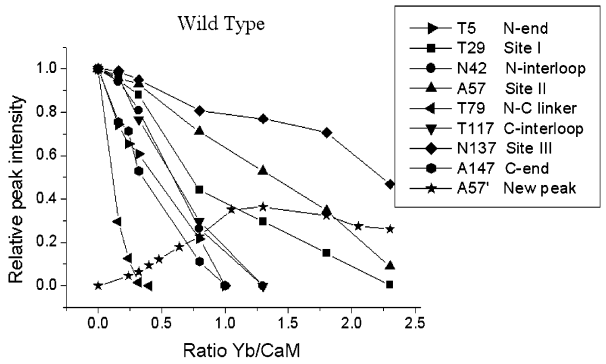
Wild Type
T5 N-end
T29 Site I
N42 N-interloop
A57 Site II
T79 N-C linker
T117 C-interloop
N137 Site III
A147 C-end
A57' New peak
Relative peak intensity
Ratio Yb/CaM

A

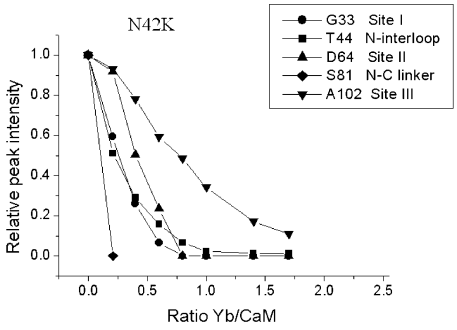
N42K
G33 Site I
T44 N-interloop
D64 Site II
S81 N-C linker
A102 Site III
Relative peak intensity
Ratio Yb/CaM

B

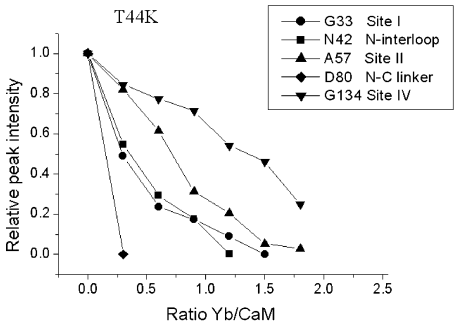
T44K
G33 Site I
N42 N-interloop
A57 Site II
D80 N-C linker
G134 Site IV
Relative peak intensity
Ratio Yb/CaM

C

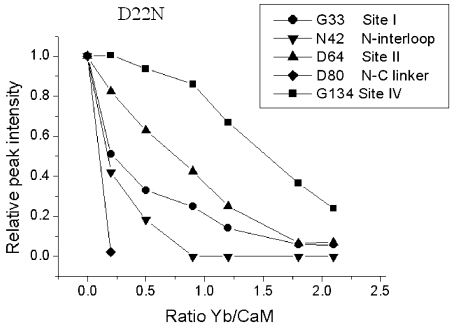
D22N
G33 Site I
N42 N-interloop
D64 Site II
D80 N-C linker
G134 Site IV
Relative peak intensity
Ratio Yb/CaM

D

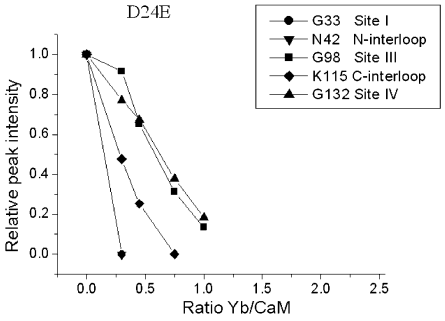
D24E
G33 Site I
N42 N-interloop
G98 Site III
K115 C-interloop
G132 Site IV
Relative peak intensity
Ratio Yb/CaM

E

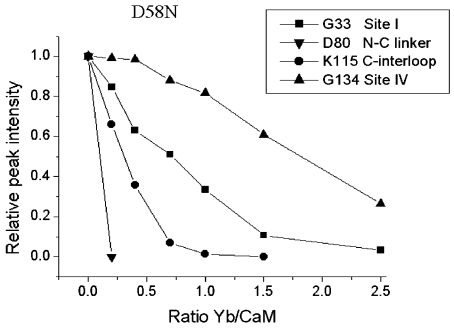
D58N
G33 Site I
D80 N-C linker
K115 C-interloop
G134 Site IV
Relative peak intensity
Ratio Yb/CaM

F

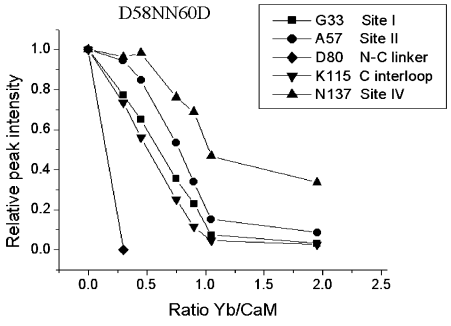
D58NN60D
G33 Site I
A57 Site II
D80 N-C linker
K115 C interloop
N137 Site IV
Relative peak intensity
Ratio Yb/CaM

G

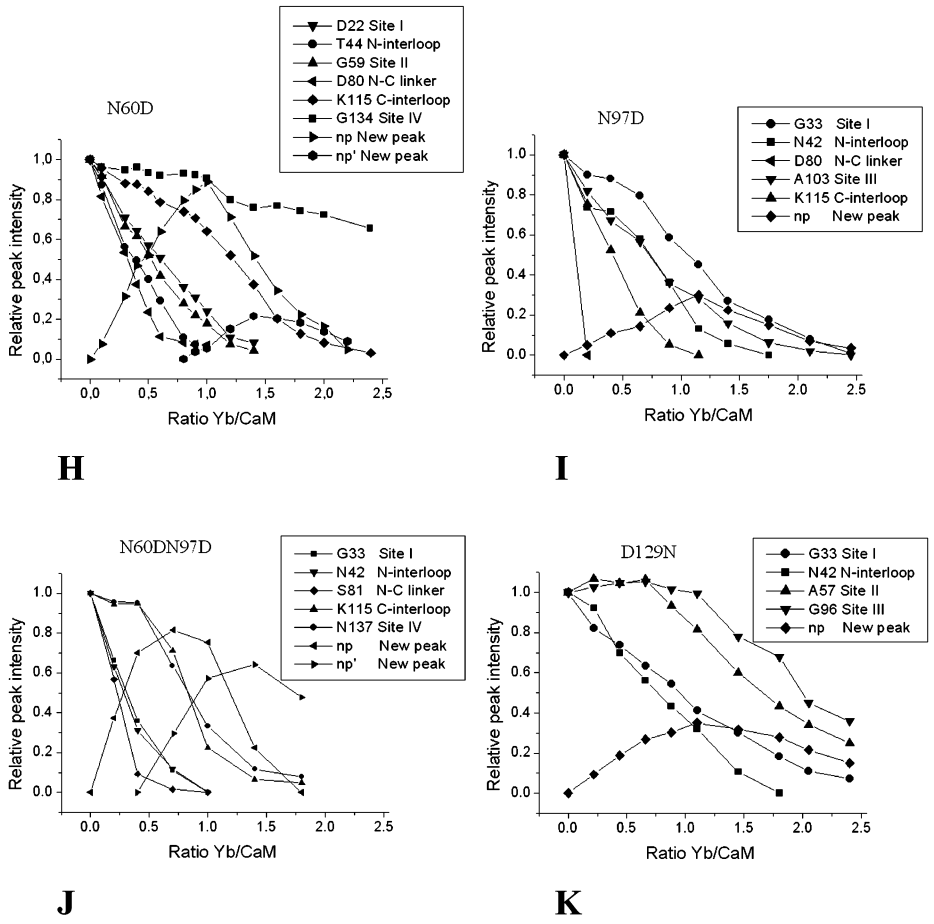

FIGURE 2: Changes in intensity of selected ^{1}H-^{15}N HSQC peaks upon titration with Yb^{3+} of WT CaM (A) and of its 10 mutants (B−K).

to a millimolar protein solution, the lanthanide/calcium competition is on unequal grounds, as the concentration ratio between the two is about 1:10. A 10-fold higher affinity of the lanthanide with respect to calcium for a particular site would result in only a 50% displacement of Ca^{2+} from the site. The same reasoning applies to the noncanonical sites, whose occupation by the lanthanide depends both on the relative affinity with respect to calcium but also on how much lanthanide is sequestered by one (or more) of the canonical sites. It is clear that, while the presence of excess calcium has allowed a meaningful and detailed analysis of the apparent lanthanide affinity for all CaM sites, a different strategy should be followed when aiming at preparing a derivative selectively substituted with lanthanide at only one site. For this purpose, N60D CaM, which already shows appreciable selectivity for lanthanides at site II even in the presence of 10 mM excess calcium, was depleted of calcium and carefully titrated with up to only 3 equivalents of Ca^{2+}. As expected (*48*, *49*), the C-terminal sites were fully occupied, while a heterogeneous distribution of calcium over the N-terminal sites was obtained (Figure 3A). However, addition of about 0.9 equivalents of lanthanide resulted in a well-defined HSQC spectrum essentially representing a single Ca_3-LnCaM derivative with the lanthanide selectively bound at site II. Selectively substituted derivatives could also be similarly prepared using Tb^{3+}, Dy^{3+}, and Tm^{3+} (Figure 3B−D).

DISCUSSION

The titration data described above can be easily analyzed in terms of (i) order of filling of canonical sites, (ii) changes in the free lanthanide concentration (monitored from exchange broadening at noncanonical sites), from which the weakening or strengthening of the mutated site can be deduced, and (iii) changes in the lanthanide affinity for the other sites (cooperativity).

The analysis of the WT titration constitutes the reference point. Besides the early broadening of the signals from the noncanonical sites, which indicates that none of the canonical sites has a high apparent lanthanide/calcium affinity ratio, the reporter signals from the two N-terminal sites decrease first. Their pairwise behavior is not necessarily due to positive cooperativity, because even if only one site becomes occupied by the lanthanide, the signals from the other site are sizably shifted, so original diamagnetic signals from both sites always decrease with the same rate. However, new hyperfine shifted signals appear during the titration, and information on cooperativity can be obtained from them (*28*). In the case of infinite positive cooperativity, the diamagnetic signals should decrease along the titration from 0 to 2 equivalents, while a single set of new signals (from the doubly occupied N-terminal domain) should appear and reach their maximum intensity at 2 equivalents. In the case of infinite negative cooperativity, all diamagnetic signals should disappear at $r = 1$ (because binding of the lanthanide at either site causes shifts of signals at *both* sites), two sets of new

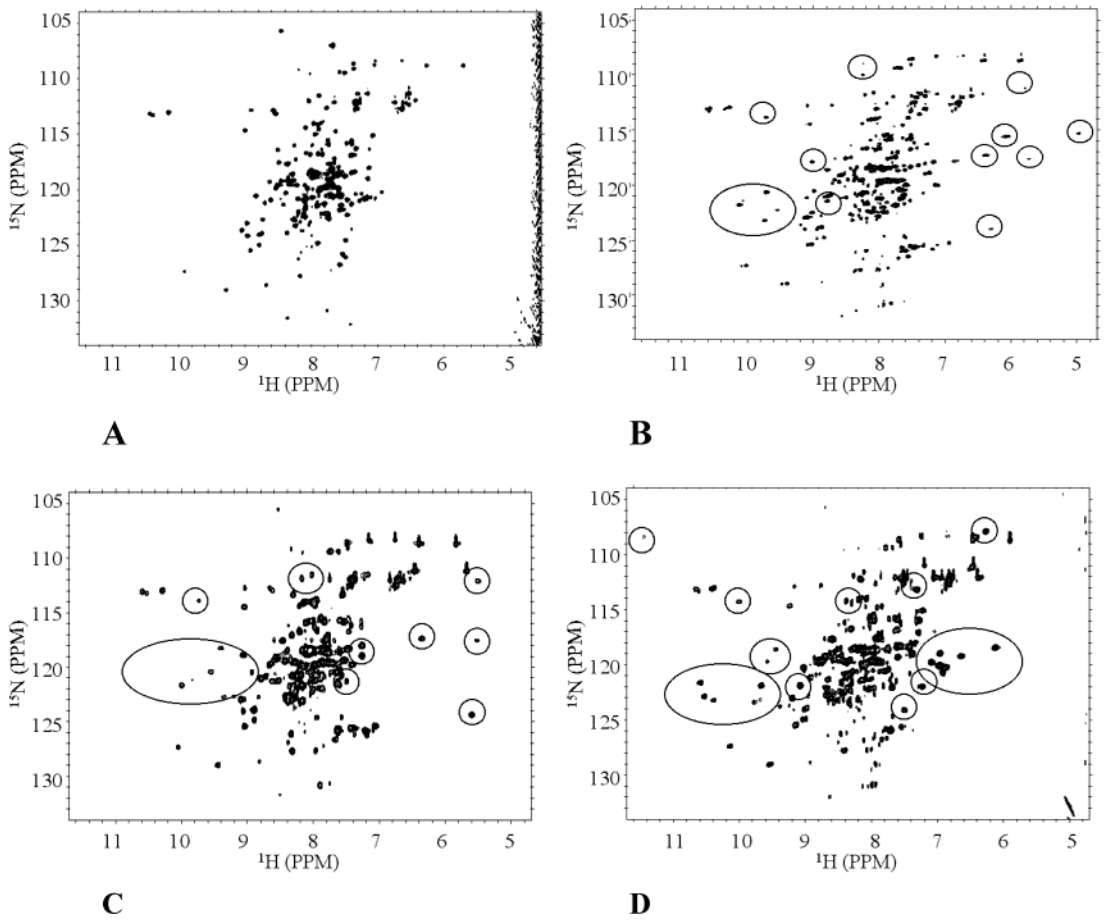

FIGURE 3: ^{1}H-^{15}N HSQC spectra of the Ca_3 N60D CaM mutant (A) and of its Ca_3Ln derivatives with Tb^{3+} (B), Dy^{3+} (C), and Tm^{3+} (D) in the absence of excess calcium. Circles represent new pseudocontact-shifted peaks.

signals (of different intensities related to the different affinities of the two sites) should appear and reach a maximum at $r = 1$, and a third set of signals from the double lanthanide derivative should start appearing at $r = 1$ and reach its maximum at $r = 2$. If one of the two sites has sizably higher affinity than the other one, then one set of intermediate signals has negligible intensity, and positive vs negative cooperativity cannot be easily discriminated. This is closest to the experimental situation, with the new set of signals reaching its maximum slightly above $r = 1$ and arising from site II, therefore pointing to site I as that preferentially occupied. The generalized broadening due to the noncanonical sites becomes more dramatic after both N-terminal sites are occupied, indicating that the affinity for the C-terminal sites is sizably smaller. The lack of new peaks from the C-terminal sites prevents the estimate of their relative affinity. Literature data suggest that site IV has the lowest lanthanide/calcium affinity ratio.

Figure 4A shows a log diagram of the apparent lanthanide/calcium affinity ratios for the four canonical sites of WT CaM. The vertical dashed line is a visual reference for the threshold to the left of which the apparent lanthanide/calcium affinity ratio for a canonical site is high enough to avoid broadening from noncanonical sites. This diagram is not intended to provide a quantitative information, but is useful to visualize the changes occurring in the various mutants and their meaning. The relative order of affinities for the various sites is estimated on the grounds of the filling order of the canonical sites, while the absolute increases or decreases of affinities of the mutated sites mainly comes from the extent of line broadening from noncanonical sites occurring along the titration. The decrease in affinity for the N-terminal sites observed for the D22N and D24E mutants (Figure 4D,E) is indicated by the increase in noncanonical line broadening in the early stages of the titration, while the reduced distance between the affinities of sites I and II comes from the different pattern of appearance and intensities of the new, paramagnetically shifted N-terminal peaks. The mutants at the inter-EF-hand loop of the N-terminal domain (N42K and T44K, Figure 4B,C) do not induce appreciable changes in the affinities of the canonical sites, as expected. The D58N mutation (Figure 4F) reduces the affinity for site II and, in doing so, also reduces the affinity for site I, apparently due to cooperativity, although the order is preserved. Conversely, the striking increase in lanthanide affinity for site II in the N60D mutant (Figure 4H) does not seem to alter the affinity for site I, as if the mutation abolished or at least reduced cooperativity in the N-terminal domain. The compensating effects of the double mutant D58N−N60D (Figure 4G) slightly increases the affinities for both N-terminal sites. N97D (Figure 4I) strongly increases the affinity of site III without increasing appreciably that of site IV (no cooperativity), and brings it slightly above that for site I. The effects of the double mutant N60D−N97D are essentially additive (Figure 4J), as expected from the lack of important cross talk between the two domains. Finally, the D129N mutation abolishes (cooperatively) the binding of lanthanides to the C-terminal site (Figure 4K).

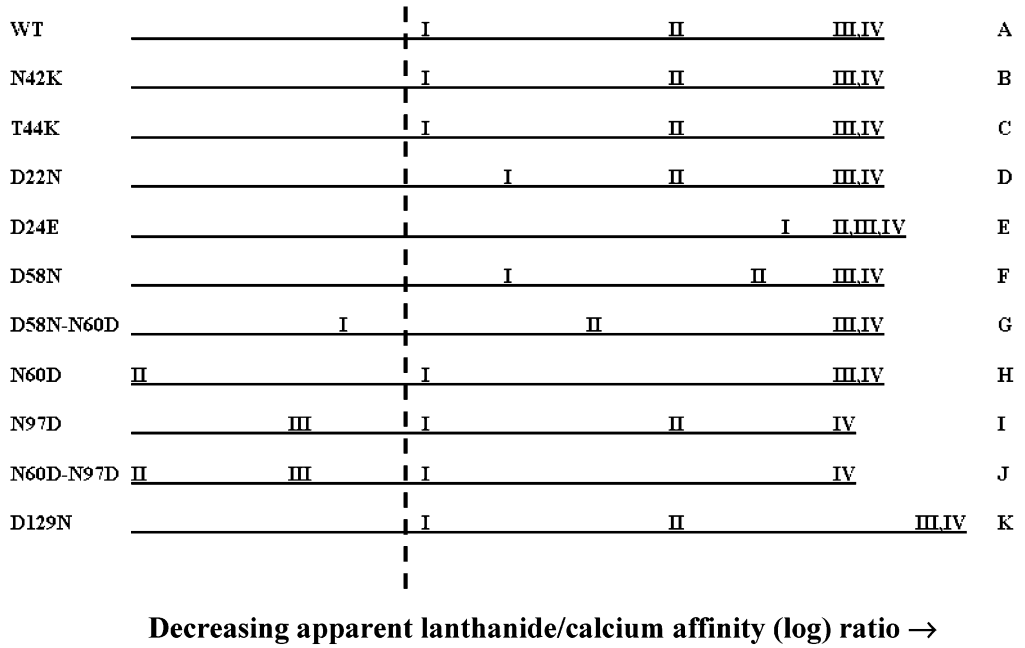

FIGURE 4: Order of the apparent lanthanide/calcium affinity (log) ratio for WT CaM and its 10 mutants described in the present work. The dashed vertical line indicates the threshold to the left of which the apparent lanthanide/calcium affinity ratio for a canonical site is high enough to avoid broadening from noncanonical sites.

Empirical Rules for a Successful Lanthanide Substitution. Some general observations can be made from the above results when viewed in the light of the known features of EF-hand sites. Calmodulin contains four canonical EF-hands, where the calcium binding loop is constituted by 12 amino acids (as opposed to the so-called pseudo EF-hands, where the loop is 14 residues long). The consensus sequence of canonical EF-hands is reported in Scheme 1. Residues 1, 3, 5, and 12 bind through one side chain oxygen, while residue 7 coordinates through the backbone carbonyl and residue 9 is hydrogen bonded to a metal-coordinated water molecule. The six donors are roughly located at the vertexes of an octahedron, i.e., along the directions of the three Cartesian axes, as shown in Scheme 1.

The only significant variability in terms of donor groups within the consensus sequence occurs at positions 3 and 5 (+Y and +Z), where either a neutral Asn or a negative Asp can be found (Scheme 1). In CaM, residues 1−3−5 are D−D−D, D−D−N, D−D−N and D−D−D in sites I, II, III, and IV, respectively. The D−N−D sequence does not occur in this protein but is found, for instance, in site II of calbindin D_{9k} (site I is a pseudo EF-hand) and in sites I and IV of other CaM-like proteins such as CaBP from *Entamoeba histolytica* (*28*, *50*). In calbindin D_9k, site II (D−N−D) has a much higher affinity for lanthanides than for calcium, while in *E. histolytica* CaBP lanthanides strongly prefer site III (D−D−D) despite the presence of two sites (I and IV) of the D−N−D type. In WT calmodulin, the present data indicate just a slight preference of lanthanides over calcium for site I (D−D−D), while site IV (also D−D−D) seems to be the least preferred. Actually, site IV is reported to have the highest affinity for calcium (*51*, *52*). Obviously, the extra negative charge by itself is not always a sufficient determinant to increase the apparent lanthanide/calcium affinity ratio. The location of the negative charges around the metal (acid pair hypothesis) plays also a role (*53*). The D22N mutant transforms the site I sequence from D−D−D to D−N−D, i.e., the same as the high affinity lanthanide site as calbindin D_9k. However, the effect in this case is to reduce the apparent lanthanide/calcium affinity ratio for site I. On the other hand, a slight increase in affinity with respect to the WT is observed for the double mutant D58N−N60D, which transforms site II from D−D−N to D−N−D. The lanthanide affinity of site II is however boosted in the N60D mutant, which transforms it from D−D−N to D−D−D. The same mutation in site III (N97D) also increases the affinity for lanthanides, although not enough to make them bind selectively to this site under the experimental conditions chosen in this work. It is apparent that predictions of the relative lanthanide vs calcium affinities of different sites cannot be made solely on the ground of the sequence of residues 1−3−5 for each site, and that other factors must play important roles. Indeed, in the N60D−N97D mutant all sites have the same D−D−D sequence for residues 1−3−5; yet, the apparent lanthanide/calcium affinity ratio is vastly different, being II ≫ III > I ≫ IV.

In any case, an important conclusion that can be drawn from this work is that, *within a given site, the apparent lanthanide/calcium affinity ratio increases in the order D−N−N < D−D−N < D−N−D < D−D−D.* It is also clear that any mutation that produces a "nonnatural" 1−3−5 sequence like, for instance, D24E (*52*) (transforming a D−D−D into a D−D−E sequence) or D129N (transforming a D−D−D into an N−D−D sequence), decreases dramatically the apparent lanthanide/calcium affinity ratio. Calcium affinity was also found to be reduced in a D−D−D to D−D−E mutation of site IV of calmodulin (*54*). For the present N−D−D mutated sequence, the calcium affinity is reduced so much that the C-terminal domain is even partially unfolded.

It is worth noting that invertebrate calmodulin from octopus differs from the vertebrate in only a few residues, two of which are however relevant to the present analysis, i.e., N60D and N97D. Calcium and lanthanide binding studies on invertebrate calmodulin did not reveal any major

difference with respect to vertebrate calmodulin (*55*), while our N60D−N97D mutant clearly shows an increase in the apparent lanthanide/calcium affinity ratio for sites II and III. The different results may be due to the different experimental conditions but may also depend on the much higher sensitivity achieved with the present NMR strategy, which is based on monitoring even modest changes in relative affinities by following the line broadening effects on the noncanonical sites.

ACKNOWLEDGMENT

Thanks are expressed to Sture Forsén and Michael Akke for the kind gift of the recombinant pRCB1 WT CaM plasmid and for several discussions and suggestions. I.G. acknowledges the support of a EC Marie Curie Grant (contract no. HPMT-CT-2000-00137).

REFERENCES

1. Kawasaki, K., and Kretsinger, R. H. (1994) Calcium-binding proteins 1: EF-hands. *Protein 1*, 343−517.
2. Ikura, M., and Ames, J. B. (2003) The role of calcium-binding proteins in the control of transcription: structure to function. *Bioessays 24*, 625−636.
3. Doanto, R., Haiech, J., Heizmann, C. W., and Gerke, V. (2000) in *Calcium*: *The Molecular Basis of Calcium Action in Biology and Medicine*, Kluwer Academic Publisher, Norwell, MA.
4. Carafoli, E. (2002) Calcium signaling: a tale for all seasons. *Proc. Natl. Acad. Sci. U.S.A. 99*, 1115−1122.
5. Thayer, S. A., Hirning, L. D., and Miller, R. J. (1988) The role of caffeine-sensitive calcium stores in the regulation of the intracellular free calcium concentration in rat sympathetic neurons in vitro. *Mol. Pharmacol. 34*, 664−673.
6. Trouslard, J., Marsh, S. J., and Brown, D. A. (1993) Calcium entry through nicotinic receptor channels and calcium channels in cultured rat superior cervical ganglion cells. *J. Physiol. 468*, 53−71.
7. Cheng, H., Lederer, W. J., and Cannell, M. B. (1993) Calcium sparks: elementary events underlying excitation-contraction coupling in heart muscle. *Science 290*, 740−744.
8. Toth, P. T., and Miller, R. J. (1995) Calcium and sodium currents evoked by action potential waveforms in rat sympathetic neurones. *J. Physiol. 485*, 43−57.
9. Rogers, M., and Dani, J. A. (1995) Comparison of quantitative calcium flux through NMDA, ATP, and ACh receptor channels. *Biophys. J. 68*, 501−506.
10. Berridge, M. J. (1995) Calcium signaling and cell proliferation. *Bioessays 17*, 491−500.
11. Ledo, F., Kremer, L., Mellstrom, B., and Naranjo, J. R. (2002) Ca^{2+}-dependent block of CREB−CBP transcription by repressor DREAM. *EMBO J. 21*, 4583−4592.
12. Peersen, O. B., Madsen, T. S., and Falke, J. J. (1997) Intermolecular tuning of calmodulin by target peptides and proteins: differential effects on Ca^{2+} binding and implications for kinase activation. *Protein Sci. 6*, 794−807.
13. Mattson, M. P., Rychlik, B., Chu, C., and Christakos, S. (1991) Evidence for calcium-reducing and excito-protective roles for the calcium-binding protein calbindin-D_{28k} in cultured hippocampal neurons. *Neuron 6*, 41−51.
14. Terentyev, D., Viatchenko-Karpinski, S., Valdivia, H. H., Escobar, A. L., and Gyorke, S. (2002) Luminal Ca^{2+} controls termination and refractory behavior of Ca^{2+}-induced Ca^{2+} release in cardiac myocytes. *Circ. Res. 91*, 414−420.
15. Toyoshima, C., Nakasako, M., Nomura, H., and Ogawa, H. (2000) Crystal structure of the calcium pump of sarcoplasmic reticulum at 2.6 A resolution. *Nature 405*, 647−655.
16. Shapiro, L., Fannon, A. M., Kwong, P. D., Thompson, A., Lehmann, M. S., Legrand, J. F., Als-Nielsen, J., Colman, D. R., and Hendrickson, W. A. (1995) Structural basis of cell−cell adhesion by cadherins. *Nature 374*, 327−337.
17. Buxbaum, J. D., Choi, E. K., Luo, Y., Lilliehook, C., Crowley, A. C., Merriam, D. E., and Wasco, W. (1998) Calsenilin: a calcium-binding protein that interacts with the presenilins and regulates the levels of a presenilin fragment. *Nat. Med. 4*, 1177−1181.
18. Dolmetsch, R. E., Pajvani, U., Fife, K., Spotts, J. M., and Greenberg, M. E. (2001) Signaling to the nucleus by an L-type calcium channel-calmodulin complex through the MAP kinase pathway. *Science 294*, 333−339.
19. Bruno, J., Horrocks, W. D., Jr., and Beckingham, K. (1996) Characterization of Eu(III) binding to a series of calmodulin binding site mutants using laser-induced Eu(III) luminescence spectroscopy. *Biophys. Chem. 63*, 1−16.
20. Sudnick, D. R., and Horrocks, W. D., Jr. (1979) Lanthanide ion probes of structure in biology. Environmentally sensitive fine structure in laser-induced terbium(III) luminescence. *Biochim. Biophys. Acta 578*, 135−144.
21. Lee, L., and Sykes, B. D. (1983) Use of lanthanide-induced nuclear magnetic resonance shifts for determination of protein structure in solution: EF calcium binding site of Carp Parvalbumin. *Biochemistry 22*, 4366−4373.
22. Geraldes, C. F. (1993) Lanthanide shift reagents. *Methods Enzymol. 227*, 43−78.
23. Bertini, I., Luchinat, C., and Rosato, A. (1996) The solution structure of paramagnetic metalloproteins, *Prog. Biophys. Mol. Biol. 66*, 43−80.
24. Bentrop, D., Bertini, I., Cremonini, M. A., Forsén, S., Luchinat, C., and Malmendal, A. (1997) The solution structure of the paramagnetic complex of the N-terminal domain of calmodulin with two Ce^{3+} ions by ^1H NMR. *Biochemistry 36*, 11605−11618.
25. Bertini, I., Donaire, A., Jimenez, B., Luchinat, C., Parigi, G., Piccioli, M., and Poggi, L. (2001) Paramagnetism-based versus classical constraints: an analysis of the solution structure of Ca Ln calbindin D_{9k}. *J. Biomol. NMR 21*, 85−98.
26. Barbieri, R., Bertini, I., Cavallaro, G., Lee, Y. M., Luchinat, C., and Rosato, A. (2002) Paramagnetically induced residual dipolar couplings for solution structure determination of lanthanide-binding proteins. *J. Am. Chem. Soc. 124*, 5581−5587.
27. Geraldes, C. F. G. C., and Luchinat, C. (2003) Lanthanides as shift and relaxation agents in elucidating the structure of proteins and nucleic acids. *Met. Ions Biol. Syst. 40*, 513−588.
28. Atreya, H. S., Mukherjee, S., Chary, K. V. R., Lee, Y.-M., and Luchinat, C. (2003) Structural basis for the sequential displacement of Ca^{2+} by Yb^{3+} in a protozoan EF-hand calcium binding protein. *Protein Sci. 12*, 412−425.
29. Horrocks, W. D., Jr., and Tingey, J. M. (2003) Time-resolved europium(III) luminescence excitation spectroscopy: characterization of calcium-binding sites of calmodulin. *Biochemistry 27*, 413−419.
30. Barbato, G., Ikura, M., Kay, L. E., Pastor, R. W., and Bax, A. (1992) Backbone dynamics of calmodulin studied by ^{15}N relaxation using inverse detected two-dimensional NMR spectroscopy; the central helix is flexible. *Biochemistry 31*, 5269−5278.
31. Lee, L., and Sykes, B. D. (1981) Proton nuclear magnetic resonance determination of the sequential ytterbium replacement of calcium in carp parvalbumin. *Biochemistry 20*, 1156−1162.
32. Biekofsky, R. R., Muskett, F. W., Schmidt, J. M., Martin, S. R., Browne, J. P., Bayley, P. M., and Feeney, J. (1999) NMR approaches for monitoring domain orientations in calcium-binding proteins in solution using partial replacement of Ca^{2+} by Tb^{3+}. *FEBS Lett. 460*, 519−526.
33. Waltersson, Y., Linse, S., Brodin, P., and Grundstrom, T. (1993) Mutational effects on the cooperativity of Ca^{2+} binding in calmodulin. *Biochemistry 32*, 7866−7871.
34. Studier, F. W., Rosenberg, A. H., Dunn, J. J., and Dubendorff, J. W. (1990) Use of T7 RNA polymerase to direct expression of cloned genes. *Methods Enzymol. 185*, 60−89.
35. Sambrook, J., Fritsch, E. F., and Maniatis, T. (1989) in *Molecular Cloning: A Laboratory Manual*. Cold Spring Harbor Laboratory Press, New York.
36. Cai, M., Huang, Y., Sakaguchi, K., Clore, G. M., Gronenborn, A. M., and Craigie, R. (1998) An efficient and cost-effective isotope labeling protocol for proteins expressed in *Escherichia coli*. *J. Biomol. NMR 11*, 97−102.
37. Gaberc-Porekar, V., and Menart, V. (2001) Perspectives of immobilized-metal affinity chromatography. *J. Biochem. Biophys. Methods 49*, 335−360.

38. Wang, C. L., Aquaron, R. R., Leavis, P. C., and Gergely, J. (1982) Metal-binding properties of calmodulin. *Eur. J. Biochem. 124*, 7−12.
39. Goddard, T. D., and Kneller, D. G. SPARKY 3, University of California, San Francisco. 2000. Computer Program.
40. Mulqueen, P., Tingey, J. M., and Horrocks, W. D., Jr. (1985) Characterization of lanthanide (III) ion binding to calmodulin using luminescence spectroscopy. *Biochemistry 24*, 6639−6645.
41. Zhang, M., Tanaka, T., and Ikura, M. (1995) Calcium-induced conformational transition revealed by the solution structure of apo calmodulin. *Nat. Struct. Biol. 2*, 758−767.
42. Biekofsky, R. R., Martin, S. R., Browne, J. P., Bayley, P. M., and Feeney, J. (1998) Ca^{2+} coordination to backbone carbonyl oxygen atoms in Calmodulin and other EF-hand proteins: ^{15}N chemical shifts as probes for monitoring individual-site Ca^{2+} coordination. *Biochemistry 37*, 7617−7629.
43. Malmendal, A., Evenäs, J., Forsén, S., and Akke, M. (1999) Structural dynamics in the C-terminal domain of calmodulin at low calcium levels. *J. Mol. Biol. 293*, 883−899.
44. Allegrozzi, M., Bertini, I., Janik, M. B. L., Lee, Y.-M., Liu, G., and Luchinat, C. (2000) Lanthanide induced pseudocontact shifts for solution structure refinements of macromolecules in shells up to 40 A from the metal ion, *J. Am. Chem. Soc. 122*, 4154−4161.
45. Bertini, I., Luchinat, C., and Parigi, G. (2001) in *Solution NMR of Paramagnetic Molecules*, Elsevier, Amsterdam.
46. Ikura, M., Kay, L. E., and Bax, A. (1990) A novel approach for sequential assignment of ^{1}H, ^{13}C and ^{15}N spectra of larger proteins: heteronuclear triple-resonance three-dimensional NMR spectroscopy. Application to calmodulin. *Biochemistry 29*, 4659−4667.
47. Evenäs, J., Malmendal, A., Thulin, E., Carlström, G., and Forsén, S. (1998) Ca^{2+} binding and conformational changes in a calmodulin domain. *Biochemistry 37*, 13744−13754.
48. Rawas, A., Moreton, K., Muirhead, H., and Williams, J. (1989) Preliminary crystallographic studies on duck ovotransferrin. *J. Mol. Biol. 208*, 213-214.
49. Evenäs, J., Forsén, S., Malmendal, A., and Akke, M. (1999) Backbone dynamics and energetics of a calmodulin domain mutant exchanging between closed and open conformations. *J. Mol. Biol. 289*, 603−617.
50. Atreya, H. S., Sahu, S. C., Bhattacharya, A., Chary, K. V. R., and Govil, G. (2001) NMR derived solution structure of an EF-hand calcium-binding protein from Entamoeba Histolytica. *Biochemistry 40*, 14392−14403.
51. VanScyoc, W. S., Sorensen, B. R., Rusinova, E., Laws, W. R., Ross, J. B., and Shea, M. A. (2002) Calcium binding to calmodulin mutants monitored by domain-specific intrinsic phenylalanine and tyrosine fluorescence. *Biophys. J. 83*, 2767−2780.
52. Wu, X., and Reid, B. R. (1997) Structure/calcium affinity relationships of site III of calmodulin: testing the acid pair hypothesis using calmodulin mutants. *Biochemistry 36*, 8649−8656.
53. Henzl, M. T., Hapak, R. C., and Goodpasture, E. A. (1996) Introduction of a fifth carboxylate ligand heightens the affinity of the oncomodulin CD and EF sites for Ca^{2+}. *Biochemistry 35*, 5856−5869.
54. Wu, X., and Reid, R. E. (1997) Conservative D133E mutation of calmodulin site IV drastically alters calcium binding and phosphodiesterase regulation. *Biochemistry 36*, 3608−3616.
55. Bruno, J., Horrocks, W. D., Jr., and Zauhar, R. J. (1992) Europium-(III) luminescence and tyrosine to terbium(III) energy-transfer studies of invertebrate (octopus) calmodulin. *Biochemistry 31*, 7016−7026.

BI034494Z